Proceedings of the 7th JFPS International
Symposium on Fluid Power, TOYAMA 2008
September 15-18, 2008

OS3-1

NUMERICAL MODELING OF RECIPROCATING FLUID POWER SEALS

Richard F. SALANT* and Bo YANG*

* George W. Woodruff School of Mechanical Engineering
Georgia Institute of Technology
Atlanta, Georgia 30332-0405, USA
(E-mail: richard.salant@me.gatech.edu)

ABSTRACT

A numerical model of reciprocating fluid power seals has been developed. It has been applied to a variety of hydraulic rod seals, although it could also be used to simulate hydraulic piston seals as well as pneumatic seals. The model is soft elastohydrodynamic and consists of coupled fluid mechanics, contact mechanics, deformation mechanics and thermal analyses. Results for typical rod seals show that these seals operate with mixed lubrication between the rod and seal surfaces, and that the roughness of the seal plays a major role in determining the leakage characteristics of the seal. For a given seal design and set of operating conditions there is a critical seal roughness, below which there will be zero net leakage per cycle and above which the seal will leak.

KEY WORDS

Seals, Rod seals, Soft elastohydrodynamics

NOMENCLATURE

E	*elastic modulus*
F	*cavitation index*
H	*dimensionless average film thickness, h/σ*
H_s	*static undeformed film thickness, h_s/σ*
H_T	*dimensionless average truncated film thickness, h_T/σ*
I_1	*influence coefficient for normal (radial) deformation*
L	*length of solution domain in x-direction*
P	*dimensionless fluid pressure, p/p_a*
p_a	*ambient pressure*
P_c	*dimensionless contact pressure for deformation analysis, p_c/E*
P_{def}	*dimensionless fluid pressure for deformation analysis, $P(p_a)/E$*
P_{sc}	*dimensionless static contact pressure, p_{sc}/E*
P_{sealed}	*dimensionless sealed pressured, psealed/pa*
P_t	*dimensionless total pressure, $P_{def} + P_c$*
$\hat{q}$	*dimensionless flow rate per unit circumferential length, $12\mu_0 qL/[(p_a)\sigma^3]$*
R	*asperity radius*
U	*surface speed of rod*
$\hat{x}$	*dimensionless axial coordinate, x/L*
$\hat{\alpha}$	*dimensionless pressure-viscosity coefficient, αp_a*
ϕ	*fluid pressure/density function, defined by Eqs. (2) and (3)*
$\phi_{s,c,x}$	*shear flow factor*
ϕ_{xx}	*pressure flow factor*
μ_0	*viscosity at atmospheric pressure*
$\hat{\rho}$	*dimensionless density, Δ/Δ_l*
Δ_l	*liquid density*
$\hat{\sigma}$	*dimensionless rms roughness of sealing element*

	surface, $\sigma R^{1/3}\eta^{2/3}$
ν	*Poisson's ratio*
ζ	*dimensionless rod speed,* $(\mu_0 UL)/[(p_a)\sigma^2]$
η	*asperity density*

INTRODUCTION

Fluid seals play important roles in fluid power systems, since excessive leakage can degrade performance and, most importantly, pollute the environment. The present paper is concerned with linear reciprocating seals, which are used in linear actuators as rod and piston seals. A significant amount of research on hydraulic reciprocating rod seals, both experimental and theoretical, has been performed since the 1960's, e.g. [1-13]. However, it is only in the last few years, with the advent of modern computational techniques, that it is possible to analyze the detailed behavior of these seals. While most previous theoretical studies assume that full film lubrication exists between the seal lip and the shaft, and the sealing surfaces are perfectly smooth, the present study shows that mixed lubrication occurs and the seal surface roughness plays an important role in determining whether or not a seal will leak. In the present study, a numerical model of reciprocating fluid power seals has been developed. It has been applied to a variety of hydraulic rod seals, although it could also be used to simulate hydraulic piston seals as well as pneumatic seals. In this paper, only a double lip U-cup seal is considered.

ANALYSIS

A typical double lip U-cup hydraulic rod seal is shown in Fig. 1. The rod is assumed to be perfectly smooth, while the seal lip is treated as rough. This is reasonable since during the run-in period, the rod is polished to a very smooth finish.

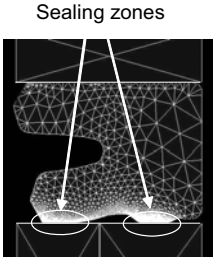

Figure 1 Rod seal

The fluid mechanics of the sealing zone is governed by the Reynolds equation. Noting that the seal is axisymmetric, and that the film thickness is very small compared to the seal radius, the flow is modeled as one-dimensional in a Cartesian coordinate system. Since cavitation may occur, the following form of Reynolds equation is used [14].

$$\frac{d}{d\hat{x}}\left[\phi_{xx}H^3 e^{-\hat{\alpha}F\phi}\frac{dF\phi}{d\hat{x}}\right] = 6\zeta\left[\frac{d}{d\hat{x}}\left\{\left[1+(1-F)\phi\right]H_T\right\}+F\frac{d\phi_{s.c.x}}{d\hat{x}}\right] \tag{1}$$

In the liquid region,

$$\phi \geq 0 \quad F = 1 \text{ and } P = \phi \tag{2}$$

In the cavitated region,

$$\phi < 0 \quad F = 0 \text{ and } P = 0,\ \hat{\rho} = 1+\phi \tag{3}$$

For the primary and secondary lips, the boundary conditions are,

$$\begin{aligned} \phi_{primary} &= P_{sealed} \quad at\ \hat{x} = 0 \\ &= \phi_{interlip} \quad at\ \hat{x} = 1 \\ \phi_{secondary} &= \phi_{interlip} \quad at\ \hat{x} = 0 \\ &= 1 \qquad at\ \hat{x} = 1 \end{aligned} \tag{4}$$

The flow factors ϕ_{xx} and $\phi_{s.c.x}$ are functions of the ratio of the film thickness to the roughness amplitude and the roughness geometry (aspect ratio and orientation of the asperities), and are obtained from [15, 16].

Equations (1)-(4) are solved for ϕ and F using a micro-control volume finite difference scheme, for given values of H, ϕ_{xx} and $\phi_{s.c.x}$, using the tri-diagonal matrix algorithm (TDMA). This yields the pressure distribution and the location of cavitation zones.

Once ϕ and F are obtained, the flow rate (per unit circumferential length) through the film (giving the instantaneous leakage rate) can be found from,

$$\hat{q} = -\phi_{xx}e^{-\hat{\alpha}F\phi}H^3\frac{dF\phi}{dx} + 6\zeta\left\{\left[1+(1-F)\phi\right]H_T + F\phi_{s.c.x}\right\} \tag{5}$$

The flow rates past the two lips must be equal.

Since significant asperity contact may occur (mixed lubrication), it is necessary to add an asperity contact pressure to the hydrodynamic pressure in computing the normal deformation and film thickness. This contact pressure is computed using the Greenwood and Williamson surface contact model [17]. Assuming a Gaussian distribution of asperities,

$$P_c = \frac{4}{3}\frac{1}{\left(1-\nu^2\right)}\hat{\sigma}^{\frac{3}{2}}\frac{1}{\sqrt{2\pi}}\int_H^{\infty}\left(z-H\right)^{\frac{3}{2}}e^{-\frac{z^2}{2}}dz \qquad (6)$$

To compute the film thickness distribution, it is necessary to compute the radial (normal) deformation of the sealing element. Since this will be done within an iteration loop, it is necessary to use a computationally efficient method. The influence coefficient method has been chosen. With this method it is recognized that the deformation at any location is proportional to the forces applied at every location. Thus, in discretized form with n axial nodes across the sealing zone, the film thickness at the ith node can be expressed as,

$$H_i = H_s + \sum_{k=1}^{n} (I_1)_{ik}(P_t - P_{sc})_k \qquad (7)$$

The proportionality factors $(I_1)_{ik}$, the "influence coefficients," are computed off-line using a commercial finite element analysis code. Thus, the on-line model contains only linear algebraic equations. The pressure Pt is the sum of the fluid pressure and the contact pressure due to contacting asperities. P_{sc} is the static contact pressure distribution, also computed off-line with a commercial finite element analysis code.

The static film thickness, H_s, is computed by equating the static contact pressure obtained from the finite element analysis for smooth surfaces under pressurized conditions, P_{sc}, with the contact pressure distribution computed from Eq. (6) under static conditions [18].

In some computations, a thermal analysis is also included. It involves an analytical solution to the classical thermal conduction equation for a moving heat source, treating the rod as a semi-infinite body and neglecting heat transferred into the seal. Heat generation through both viscous friction and contact friction is accounted for. The computed interface temperature is used to evaluate the fluid viscosity in the sealing zone.

Since the equations discussed above are strongly coupled, it is necessary to use an iterative computational procedure, as shown in Fig. 2.

RESULTS

Injection Molding Application

Computations have been performed for a typical seal in an injection molding application, with base parameters of: E = 43 x 10^6 Pa, ν = 0.49, p_{sealed} = 6.90 MPa (1000 psi), U = 0.635 m/s (25 in/s) outstroke, U = -0.813 m/s (-32 in/s) instroke, μ_0 = 0.043 Pa s, α = 20 x 10^{-9} Pa^{-1},

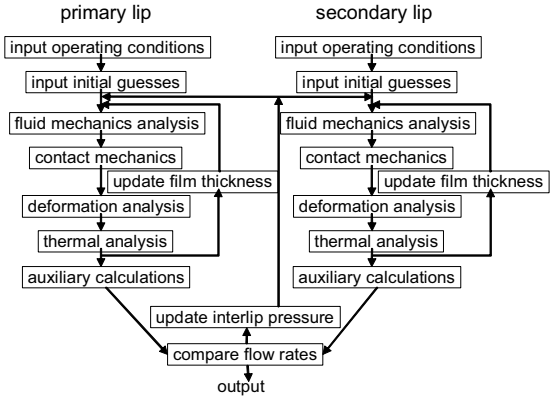

Figure 2 Computational procedure

R = 1.0 μm, η = 10^{14} m^{-2}, f = 0.25, rod diameter = 88.9 mm (3.5 in), stroke length = 1.93 m (76 in), seal width = 6.8 mm (0.27 in). The seal roughness is assumed to be isotropic. As pointed out in the Analysis section, the rod is treated as perfectly smooth.

Figure 3 contains a plot of the fluid transport during outstroke and instroke for the double lip seal. (The fluid transport past the secondary seal is the same as that past the primary seal, since this is a steady state analysis.) As can be seen, the difference between the fluid transport during outstroke and instroke, the net leakage per cycle, is strongly dependent on the seal roughness. For zero net leakage, the instroke fluid transport must exceed the outstroke transport. This occurs at values of rms seal roughness below a critical roughness of approximately 0.3 μm. For higher values of roughness, this seal will leak at the given operating conditions.

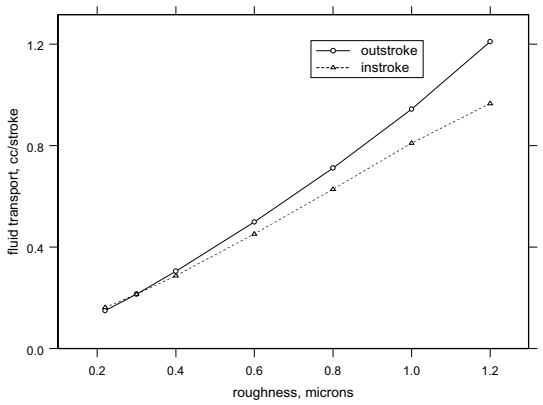

Figure 3 Fluid transport vs. seal roughness

From Fig. 3 it is seen that a seal with a roughness of 0.22 μm is non-leaking. Figure 4 shows the film thickness distributions under the primary lip during

outstroke and instroke, for such a seal. These indicate that mixed lubrication exist, since the film thickness is less than 3σ. It is also seen that the film thickness is larger during the instroke than during the outstroke. This promotes effective sealing, since it reduces the resistance to flow during the instroke compared to the outstroke.

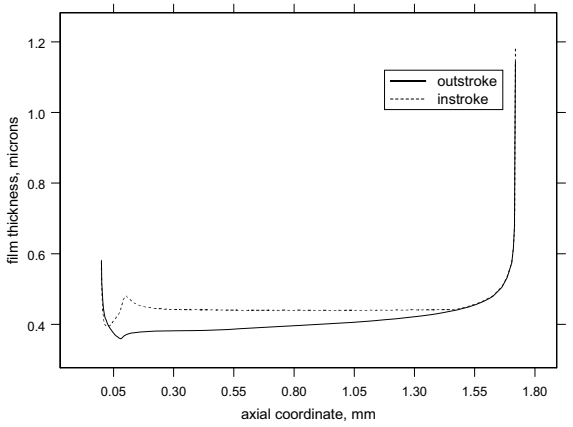

Figure 4 Film thickness distribution, primary lip, σ = 0.22 μm

The film thickness distribution under the primary lip for a leaking seal, with a roughness of 0.6 μm, is shown in Fig. 5. Here, again, mixed lubrication exists. However in this case the sealing zone is shorter during the outstroke than during the instroke (due to an elevated interlip pressure), and the film thickness during the instroke and outstroke have about the same values at corresponding locations. This is a less favorable characteristic, compared to the non-leaking seal.

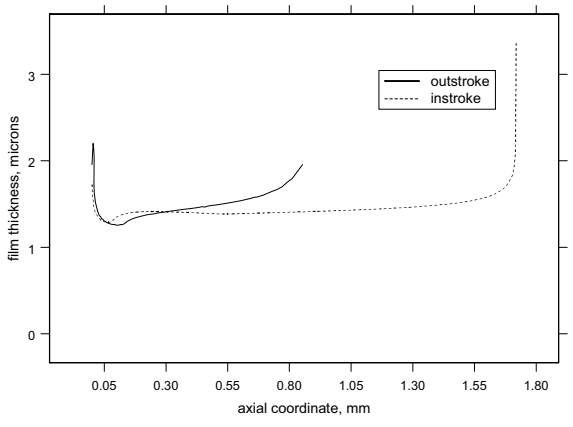

Figure 5 Film thickness distribution, primary lip, σ = 0.60 μm

Figure 6 shows the static contact pressure, dynamic contact pressure and fluid pressure distributions under the primary lip for the non-leaking seal during the outstroke. The fluid pressure is zero over a large portion of the sealing zone, indicating the occurrence of cavitation. This is a favorable characteristic, since cavitation restricts the flow of fluid out of the cylinder.

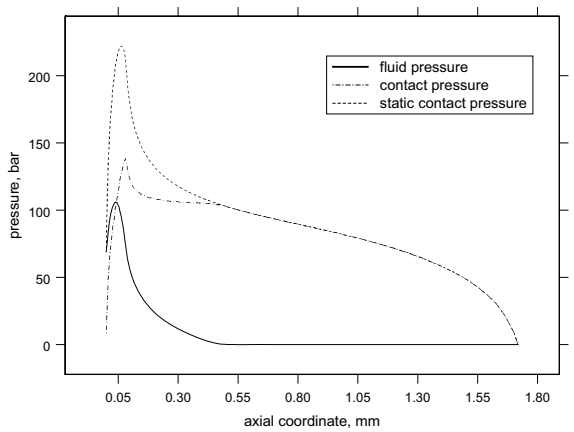

Figure 6 Pressure distributions, primary lip, σ = 0.22 μm, outstroke

The pressure distributions for the same seal during the instroke are shown in Fig. 7. Here it is seen that the extent of cavitation has been greatly reduced. This is favorable, since cavitation during the instroke tends to prevent fluid from being drawn back into the cylinder.

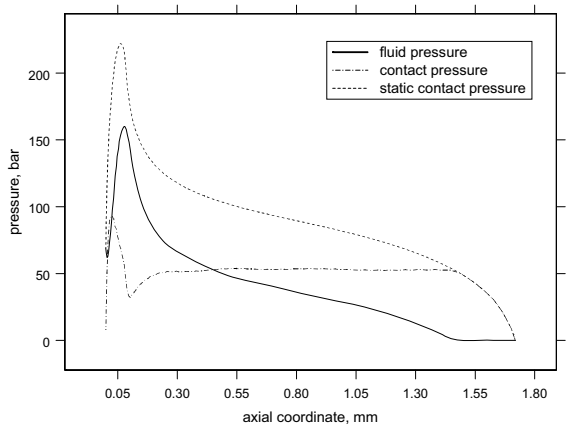

Figure 7 Pressure distributions, primary lip, σ = 0.22 μm, instroke

Figures 8 and 9 contain the corresponding outstroke and instroke pressure distributions for the leaking seal. The behavior is opposite to that of the non-leaking seal. During the outstroke there is no cavitation, allowing unrestrained flow out of the cylinder, while during the instroke there is extensive cavitation, tending to prevent fluid from being drawn back into the cylinder.

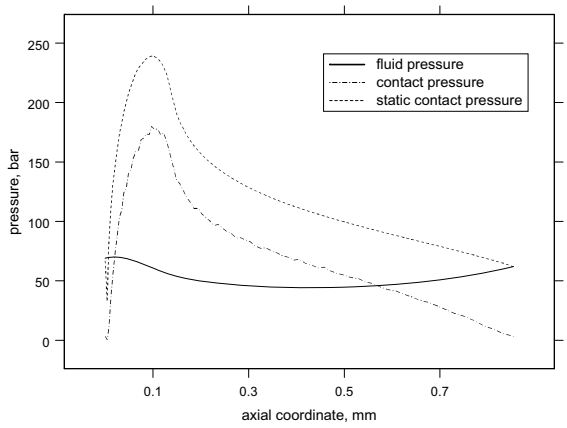

Figure 8 Pressure distributions, primary lip, σ = 0.60 μm, outstroke

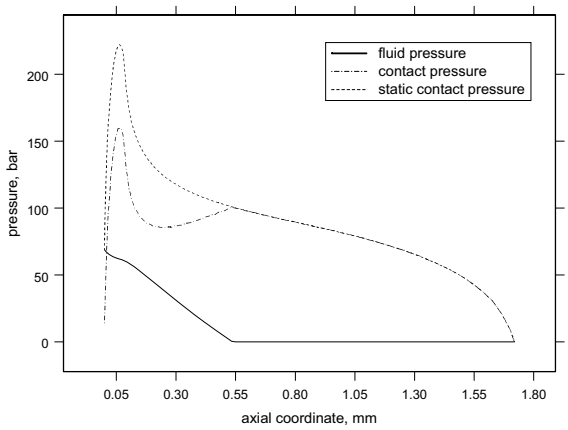

Figure 9 Pressure distributions, primary lip, σ = 0.60 μm, instroke

Conventional Actuator

In the above injection molding application, the sealed pressure is the same during the outstroke and the instroke (6.90 MPa). Computations have also been performed for a conventional actuator in which the sealed pressure is ambient during the outstroke and a range of specified values during the instroke. The seal has the same geometry as that in the injection molding application but is smaller, with a rod diameter of 44 mm (1.75 in) and a stroke length of 0.23 m (9 in).

The net leakage (per cycle) versus rod speed is shown in Fig. 10 for a sealed pressure of 6.90 MPa (1000 psi) and varying roughness. The leakage is highest at the lowest speeds; as the speed is increased the leakage decreases until the critical speed is reached, at which point there is zero leakage. At a given speed, the higher the seal roughness, the higher is the leakage.

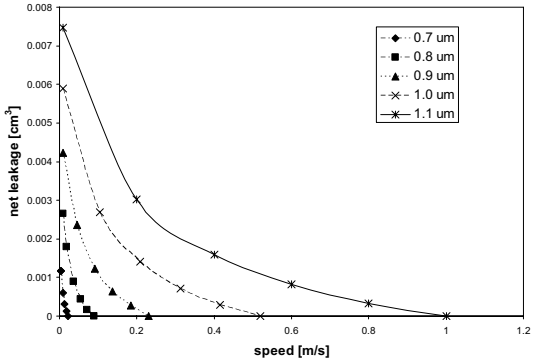

Figure 10 Leakage per cycle vs. rod speed, p_s = 6.9 MPa

Figure 11 shows a similar plot of net leakage versus rod speed, but for a seal roughness of 0.9 μm and varying sealed pressure. At a given speed, the higher the sealed pressure, the higher is the leakage. Similar to figure 4, at each sealed pressure, as the speed is increased the leakage decreases until the critical speed is reached, at which point there is zero leakage.

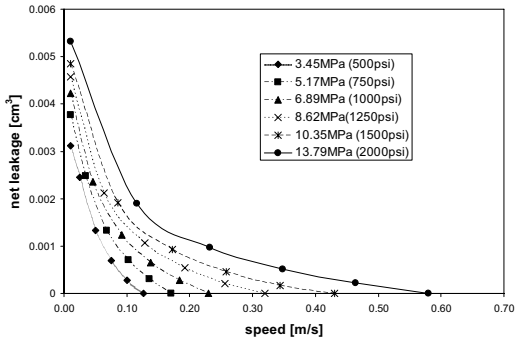

Figure 11 Leakage per cycle vs. rod speed, σ = 0.9 μm

The critical speed vs. seal roughness is shown in Fig. 12 for varying sealed pressure. It is seen that the critical speed increases with both increased roughness and increased sealed pressure.

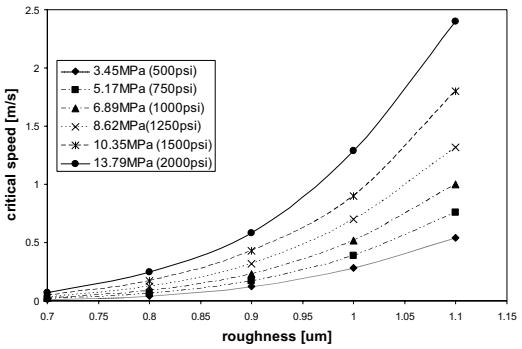

Figure 12 Critical speed vs. roughness

CONCLUSIONS

The results of this study indicate that typical rod seals operate with mixed lubrication in the interface between the rod and the seal, and the roughness of the seal surface plays a major role in determining the leakage characteristics. For a given seal design and set of operating conditions there is a critical roughness, below which there will be zero net leakage per cycle. For a given seal design, there is a critical rod speed, above which there will be zero net leakage per cycle. That critical speed is dependent on the seal roughness and sealed pressure.

The results also indicate that there are a number of characteristics that promote zero or reduced leakage in rod seals: small seal surface roughness, small lubricating film thickness, thicker film during outstroke than during instroke, cavitation in film during outstroke, and no cavitation or reduced cavitation during instroke.

ACKNOWLEDGMENTS

The authors gratefully acknowledge the financial support of the Cooperative Network for Research, National Fluid Power Association; the National Science Foundation, Engineering Research Center for Compact and Efficient Fluid Power; and the Georgia Power Company.

REFERENCES

1. Ishiwata, H. and Kambayashi, H., 1964, “A Study of Oil Seal for Reciprocating Motion,” Proc. 2nd BHRA International Conference on Fluid Sealing, B3.
2. O’Donogue, J. P. and Lawrie, J. M., 1964, “The Mechanism of Lubrication in a Reciprocating Seal,” Proc. 2nd BHRA International Conference on Fluid Sealing, B6.
3. Field, G. J. and Nau, B. S., 1974, “A Theoretical Study of the Elastohydrodynamic Lubrication of Reciprocating Rubber Seals,” ASLE Transactions, 18, pp. 48-54.
4. Müller, H. K. and Nau, B. S., 1998, Fluid Sealing Technology, Marcel Dekker, New York.
5. Hirano, F. and Kaneta, M., 1971, “Theoretical Investigation of Friction and Sealing Characteristics of Flexible Seals for Reciprocating Motion,” Proc. 5th BHRA International Conference on Fluid Sealing, G2.
6. Kanters, A. F. C., Verest, J. F. M. And Visscher, M., 1990, “On Reciprocating Elastomeric Seals: Calculation of Film Thicknesses Using the Inverse Hydrodynamic Lubrication Theory,” Tribology Transactions, 33, pp. 301-306.
7. Field, G. J., and Nau, B. S., 1973 “Film Thickness and Friction Measurements During Reciprocation of a Rectangular Section Rubber Seal Ring,” Proc. 6th BHRA International Conference on Fluid Sealing, C5.
8. Kawahara, Y., Ohtake, Y. and Hirabayashi, H., 1981, “Oil Film Formation of Oil Seals for Reciprocating Motion,” Proc. 9th BHRA International Conference on Fluid Sealing, C2.
9. Kanters, A. F. C. and Visscher, M., 1988, “Lubrication of Reciprocating Seals: Experiments on the Influence of Surface Roughness on Friction and Leakage,” Proc. 15th Leeds-Lyon Symposium on Tribology, pp. 69-77.
10. Nikas, G. K., 2003, “Elastohydrodynamics and Mechanics of Rectangular Elastomeric Seals for Reciprocating Piston Rods,” J. of Tribology, 125, pp. 60-69.
11. Nikas, G. K, 2003, “Transient Elastohydrodynamic Lubrication of Rectangular Elastomeric Seals for Linear Hydraulic Actuators,” J. of Engineering Tribology, 217, pp. 461-473.
12. Salant, R. F., Maser, N. and Yang, B. 2007, “Numerical Model of a Reciprocating Hydraulic Rod Seal,” Journal of Tribology, 129, pp. 91-97.
13. Yang, B. and Salant, R. F. 2007, “A Numerical Model of a Reciprocating Rod Seal With a Secondary Lip,” Tribology Transactions, 51, pp. 119-127.
14. Payvar, P. and Salant, R. F., 1992, "A Computational Method for Cavitation in a Wavy Mechanical Seal," Journal of Tribology, 114, pp. 199-204.
15. Patir, N. and Cheng, H. S., 1978, “An Average Flow Model for Determining Effects of Three-Dimensional Roughness on Partial Hydrodynamic Lubrication,” J. of Lubrication Technology, 100, pp. 12-17.
16. Patir, N. and Cheng, H. S., 1979, “Application of Average Flow Model to Lubrication Between Rough Sliding Surfaces,” J. of Lubrication Technology, 101, pp. 220-229.
17. Greenwood, J. A. and Williamson, J. B. P., 1966, “Contact of Nominally Flat Rough Surfaces,” Proc. Royal Society (London), A295, pp. 300-319.
18. Streator, J. L., 2001, “A Model of Mixed Lubrication with Capillary Effects,” Proc. 15th Leeds-Lyon Symposium on Tribology, pp. 121-128.